Kinetic and Spectroscopic Evidence for an Irreversible Step between Deprotonation and Reprotonation of the Schiff Base in the Bacteriorhodopsin Photocycle†

György Váró‡ and Janos K. Lanyi*
Department of Physiology and Biophysics, University of California, Irvine, California 92717
Received November 16, 1990; Revised Manuscript Received February 22, 1991

ABSTRACT: The photocycles of wild-type bacteriorhodopsin and its D96N form were investigated with a gated multichannel analyzer. Reconstruction of the spectra of the photointermediates from the measured time-resolved difference spectra allowed evaluation of the kinetics; the data at pH 7 in the presence of 100 mM NaCl were best fitted by the scheme K ↔ L ↔ M_1 → M_2 ↔ N ↔ O → BR *plus* N → BR [Váró, G., & Lanyi, J. K. (1990) *Biochemistry 29*, 2241-2250]. The proposed two M states and the M_1 → M_2 reaction were necessitated by anomalies in the kinetics of the decay of K and L. Additional support was provided by a 4-nm blue-shift in the maximum of M in Triton X-100 solubilized bacteriorhodopsin during the photocycle; the kinetics of the shift were consistent with the time course of the proposed M_1 → M_2 transition. In the D96N mutant, the M state is stabilized, and the resulting equilibrium mixture for the intermediates could be evaluated with greater precision. The concentration ratio of L to M at the equilibrium was estimated to be no higher than 0.01. This requires the ratio of forward/reverse rates for the M_1 to M_2 conversion to be at least 200, i.e., a virtually irreversible reaction. Consistent with an earlier report, the data at lower pH and in the absence of NaCl are different and suggest the existence of a second L species; we propose that it is in equilibrium with M_2.

Illumination of the purple protein bacteriorhodopsin (BR)[1] causes the all-trans to 13-cis isomerization of its retinal chromophore (Pettei et al., 1977; Aton et al., 1977) and a sequence of thermal reactions of tens of milliseconds duration which result in the translocation of a proton across the membrane and recovery of the initial state. The intermediates of this photocycle have been identified from distinct electronic [e.g., see Lozier et al. (1975)] and vibrational [e.g., see Smith et al. (1985)] spectra which arise and decay sequentially, and are referred to as J, K, L, M, N, and O. Their absorption maxima in the visible range are at about 610, 590, 545, 410, 560, and 640 nm, respectively, while that of *all-trans*-BR is at 568 nm. It is now generally thought that in the L to M reaction the retinal Schiff base loses its proton to D85 (Braiman et al., 1988; Gerwert et al., 1989; Butt et al., 1989a; Stern et al., 1989), producing the strongly blue-shifted M species, and in the M to N reaction it regains the proton from D96 (Gerwert et al., 1989; Butt et al., 1989a; Otto et al., 1989; Tittor et al., 1989; Holz et al., 1989; Stern et al., 1989). These proton transfers constitute the principal steps in the transport. The rest of the reaction kinetics are less certain, however. A large number of different schemes have been proposed. Initially, a linear sequence containing unidirectional reactions was adopted (Lozier et al., 1975), but it is now recognized that the kinetics are more complex than predicted by this simple model (Nagle et al., 1982). Since the absorption maximum of M is greatly removed from that of BR and thus its transient formation and decay are the easiest to follow, early models concentrated on explaining the observed multiexponential M rise and decay. Some of these models postulated two or more BR species in equilibrium, each producing a photocycle with distinct M states and kinetics (Hanamoto et al., 1984; Dancsházy et al., 1988; Diller & Stockburger, 1988; Bitting et al., 1990). Other proposed a branching reaction before L in a single photocycle so as to result in two independent M states with different rise and decay (Butt et al., 1989b). In yet another recent model, a two-photon process was suggested (Kouyama et al., 1988): a second M state with different rise and decay kinetics would be produced from the photoreaction of N, an intermediate which accumulates during illumination at high pH and high salt concentration.

As the kinetics of the other intermediates were described, it became clear that many of them had complex rise and decay also. A number of current models attribute the kinetic complexities to reversible steps with back-reactions (Parodi et al., 1984) of significant rates. Thus, the N to O reaction was suggested to be reversible (Chernavskii et al., 1989; Váró et al., 1990; Gerwert et al., 1990a), as were the K to L (Váró & Lanyi, 1990a), L to M (Váró & Lanyi, 1990a,b; Alshuth & Stockburger, 1986; Ames & Mathies, 1990), and M to N (Otto et al., 1989; Váró & Lanyi, 1990b; Ames & Mathies 1990; Gerwert et al., 1990a) reactions. Two-cycle models containing only irreversible reactions were not compatible with some observations (Váró & Lanyi, 1990b). While two-cycle models containing several reversible reactions could not be rigorously ruled out, the single-cycle model with reversible reactions which has emerged from these studies was simpler and conceptually more attractive as it provided mechanistic insights into the dependencies of several of the reactions on pH (Otto et al., 1989) and humidity (Váró & Lanyi, 1990a). The temperature dependencies of the rate constants calculated after fitting such a single-cycle model also provided a self-consistent thermodynamic view of the transport process (Váró & Lanyi, 1991).

Some of the data did not quite fit the single-cycle model, however, unless another kinetic feature was introduced. The discrepancies were the following: (1) the initial part of the

† This work was supported by a grant from the National Institutes of Health (GM 29498).
‡ Permanent address: Biological Research Center of the Hungarian Academy of Sciences, Szeged, Hungary.

[1] Abbreviations: BR, bacteriorhodopsin; J, K, L, M_1, M_2, N, and O, intermediates of the bacteriorhodopsin photocycle; D96N bacteriorhodopsin, BR in which aspartate-96 is replaced with asparagine; HEPES, 4-(2-hydroxyethyl)-1-piperazineethanesulfonic acid.

0006-2960/91/0430-5008$02.50/0

L to M interconversion led to a quasi-equilibrium consistent with forward and reverse rate constants of roughly the same magnitude, but in the latter part of the reaction, the concentration of L decreased to zero at times where the concentration of M was still maximal (Váró & Lanyi, 1990a,b); (2) the relaxation time for the decay of M was longer that the rise time of N (Gerwert et al., 1990a); and (3) in BR films at 65–75% humidity, the recovery of BR was by a direct pathway from M but followed a strongly biphasic time course (Váró & Lanyi, 1990a). The simplest solution to these kinetic problems was to introduce an irreversible reaction between two M states in series (Váró & Lanyi, 1990a,b; Gerwert et al., 1990a). Thus, the decay of L, the rise of N, and in the films the recovery of BR would be limited by the rate of a postulated $M_1 \rightarrow M_2$ reaction. Two groups which described the L to M kinetics from time-resolved resonance Raman spectra (Alshuth & Stockburger, 1986; Diller & Stockburger, 1988; Ames & Mathies, 1990) had data contrary to those from the visible spectra, however. They reported that the L/M ratio approached a constant value once M reached maximal concentration and L persisted throughout the decay of M. This was particularly evident from the results in Alshuth and Stockburger (1986) and Diller and Stockburger (1988). From the constant L/M ratio, equilibration of L with a single M state was proposed.

The irreversible $M_1 \rightarrow M_2$ reaction in the middle of a series of reversible reactions, originally introduced to fit kinetic data, appears to be the critical step in the bacteriorhodopsin photocycle. Although not necessarily as an irreversible step, such a reaction has been suggested by others (Nagle & Mille, 1981; Schulten et al., 1984; Gerwert & Siebert, 1986; Henderson et al., 1990). This reaction fulfills a number of functions necessary for the transport. It is the step proposed to be the switch event by which the Schiff base changes its access from D85 communicating with the extracellular medium to D96 communicating with the cytoplasmic side. Thermodynamic analysis indicates (Váró & Lanyi, 1991) that a large free energy decrease occurs here conferring irreversibility to the reaction sequence. A large entropy decrease suggests that a protein conformational change is associated with this step. The excess free energy retained in the early part of the photocycle appears to be confined to the chromophore, causing lowering of the Schiff base pK_a and loss of its proton. It appears that at the M_1 to M_2 reaction all of the excess free energy is transferred from the chromophore to the protein. Taken together, these results suggest that the switch event has three functions: (1) to restore the original high pK_a to the deprotonated Schiff base so it becomes a proton acceptor; (2) to reorient the Schiff base in order to be reprotonated from the cytoplasmic side only; and (3) to ensure irreversibility of the proton transfer.

However, the evidence for two M states has been circumstantial. Two M conformations differing in amide band absorptions (Gerwert et al., 1985) and retinal orientations (Hasselbacher & Dewey, 1986) have been observed before. It was argued that two M states might exist which differ in the retinal C14–C15 single-bond configuration (Gerwert & Siebert, 1986) but this is disputed (Fodor et al., 1988b). Another alternative is a change in the configuration of the C=N bond. In M, this appears to be anti (Fodor et al., 1988a), but ^{13}C NMR spectra indicate that under nonphysiological conditions at least, an additional M with C=N syn configuration can be produced (Smith et al., 1989). A large number of observations [e.g., see Engelhard et al. (1985), Braiman et al. (1987), Dencher et al. (1989), and Gerwert et al. (1990b)] suggest conformational relaxations in the second half of the photocycle but do not indicate where these had begun.

In view of the importance of the proposed $M_1 \rightarrow M_2$ reaction in coupling proton transfer to retinal isomerization, and the contradictions in the results which bear on this point, the existence of this step had to be critically examined. We describe here (1) studies of the photocycle of monomeric BR and (2) the time course of the L to M reaction in BR with the single-residue replacement, D96N. Very few reports have appeared on the photoreaction of solubilized BR [e.g., see Dencher et al. (1983)]; we find that the kinetic and spectral separation of the two M species is more readily observable in this system than in purple membrane. As regards the kinetic evidence for two M species, the D96N bacteriorhodopsin is especially suited for studying the L to M reaction because the replacement of D96 with asparagine prevents the rapid intramolecular reprotonation of the Schiff base and the lifetime of M is thereby prolonged (Holz et al., 1989; Butt et al., 1989a; Tittor et al., 1989). Otherwise, the chromophore, the photocycle, and the transport appear to be relatively unaffected. Because M is stabilized, N is not produced until much later in the photocycle, and the late part of the L kinetics can be followed without interference from absorption changes due to N. The results we report here provide strong evidence for the existence of an irreversible $M_1 \rightarrow M_2$ reaction and for the proposed model. At the same time, we could confirm the results of Alshuth and Stockburger (1986) under the experimental conditions they employed. Although these had appeared to contradict the proposed model, we suggest a modification to account for the discrepancy.

Materials and Methods

Purple membranes were isolated from *Halobacterium halobium* S9 and *Halobacterium* sp. GRB strain 326 (containing a point mutation resulting in the replacement of D96 with asparagine, D96N; Soppa & Oesterhelt, 1989) as described before (Oesterhelt & Stoeckenius, 1974). The latter organism was a generous gift of D. Oesterhelt. Unless otherwise indicated, the measurements were in 100 mM NaCl/50 mM phosphate buffer, pH 7.0. Solubilization was with 2% Triton X-100 in the absence of salt. The CD spectrum in the visible (which will be shown elsewhere) indicated that after incubation for 2 days at room temperature and centrifugation to remove a small amount of unsolubilized material the BR was entirely in the monomeric state. After solubilization, 100 mM NaCl was added. All spectroscopy was at 20 °C. The samples were light-adapted before the measurements.

Time-resolved difference spectra were obtained with a gated optical multichannel analyzer after subnanosecond laser photoexcitation at 580 nm as described (Zimányi et al., 1989). As before, magic-angle polarization was used to avoid effects from chromophore reorientation. The laser repetition rate was 0.1–2 Hz depending on the longest relaxation time in the samples so as to allow sufficient time for the recovery of BR before each photoexcitation. Averaging was over 200–2000 traces. From the same data, spectra of the BR without flash excitation were also obtained; these showed that the BR did not change optically during the flash regimes.

Results

Effects of Solubilization on the Bacteriorhodopsin Photocycle. Figure 1 shows measured time-resolved difference spectra between 100 ns and 600 ms after photoexcitation of BR in two-dimensional crystalline arrays (purple membrane) and in solubilized monomeric form (Triton X-100 micelles).

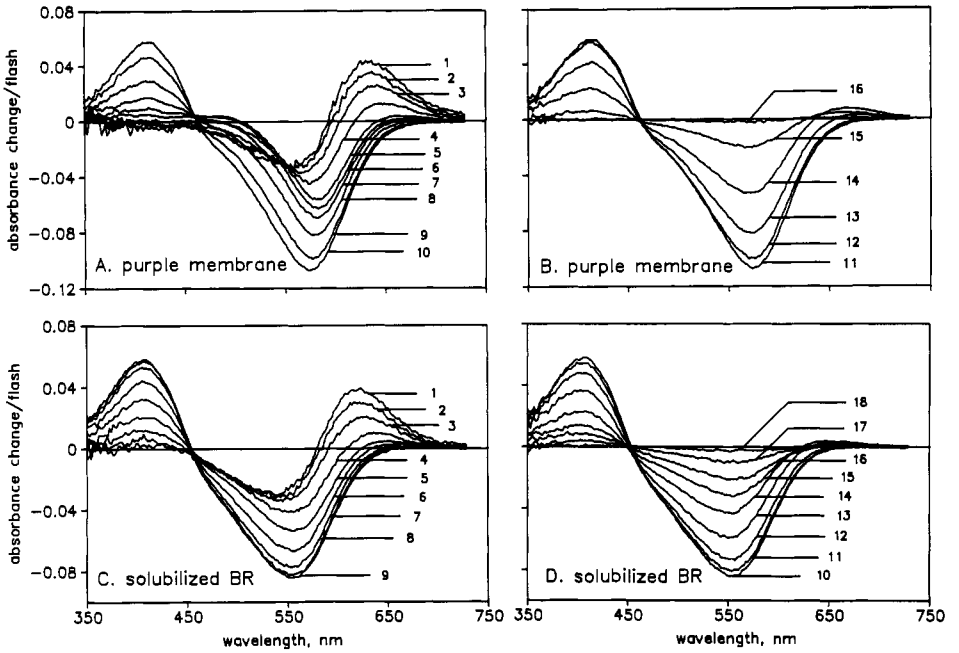

FIGURE 1: Measured time-resolved difference spectra for bacteriorhodopsin in purple membranes (A and B) and in Triton X-100 micelles (C and D). Delay times after photoexcitation are indicated by numbers. From 1 through 18, these were 100 ns, 250 ns, 600 ns, 1.5 μs, 4 μs, 10 μs, 25 μs, 60 μs, 150 μs, 400 μs, 1 ms, 2.5 ms, 6 ms, 15 ms, 40 ms, 250 ms, and 600 ms. Conditions for A: 40 nmol/mL BR in 100 mM NaCl/50 mM phosphate buffer at pH 7.0. Conditions for B: 45 nmol/mL BR, 2% Triton X-100, 100 mM NaCl, and 50 mM phosphate, pH 7.0. Both measurements were at 20 °C. Optical path length, 4 mm.

It is evident that the nature and time course of the absorption changes are different in the two samples. For example, early in the photocycle, the positive feature near 500 nm due to the L state, which develops between 1 and 5 μs, is much more pronounced in purple membranes than in the monomeric BR (compare panels A and C of Figure 1). Likewise, at the end of the photocycle, the positive feature near 650 nm, due to the O state, is more evident in purple membrane than in the monomeric BR (compare panels B and D of Figure 1). The maximum near 410 nm is due to the M intermediate. In the purple membranes, its position is independent of the delay time. Interestingly, in the solubilized samples, the maximum shifted noticeably toward the blue between 10 μs and 1 ms. The average of six maxima between 1 and 10 μs was at 406.9 nm (s^2 = 0.542), and between 1 and 10 ms at 402.5 nm (s^2 = 0.500). Analysis by *t*-test statistics indicated that the difference between the means was highly significant: 4.4 ± 1.3 nm at the 99% confidence level. Analysis of the same six early and six late difference spectra in purple membranes gave averages of 410.9 nm (s^2 = 0.642) and 410.4 nm (s^2 = 0.542), respectively, and the difference between the means was not significant: 0.5 ± 1.4 nm at the 99% confidence level.

As described previously (Vârô & Lanyi, 1990a), spectra such as these were used to first reconstruct the difference spectra of the photocycle intermediates and then to derive their time-dependent concentrations. The procedure we followed was to fit five of the difference spectra to five linear equations with adjustable parameters for the amounts of intermediates present and BR depleted until the resulting spectra for the five photointermediates obeyed the following criteria: nonnegative absorption, single peaks, shapes which resembled the predicted skewed spectra for rhodopsin-type pigments, and agreement of the positions of the maxima with the predictions of reported ethylenic stretch frequencies. The requirement that each displayed spectrum simultaneously satisfy these criteria proved to be stringent and severly restricted the choice of the variable parameters (to within 1–2% of their optimal values). Since the spectrum of M in the solubilized samples was not time-invariant, here we used six difference spectra for the calculations. We assumed that there is an early M state which is maximally red-shifted and a late M state which is maximally blue-shifted, and chose the six spectra so that the first three would contain M_1 and the second three M_2. Attempts to derive a single M spectrum were not successful because they left a sharp feature in the calculated spectra, characteristic of the difference between the spectra of the early and late M states. Thus, for the solubilized samples, we calculated two spectra for M.

The calculated absorption spectra for K, L, M, N, and O in the two kinds of BR samples are shown in Figure 2A,B. In purple membranes, the spectra agree well with the criteria listed above, and are virtually identical with earlier spectra from BR films where they are discussed in detail (Vârô & Lanyi, 1990a). A blue-shift in the BR spectrum to 552 nm and a decrease of the extinction by 20% upon solubilization, as we found, are well-known (Dencher & Heyn, 1978), but the wavelengths of the maxima of the photointermediates are not available from independent measurements. Since this criterion, important for evaluating the spectra of N and O (Vârô & Lanyi, 1990a), is missing, the spectra of these states in solubilized BR must be regarded as approximations. An interesting internal consistency is that after solubilization the absorption maxima of both all-trans states (BR and O) are considerably blue-shifted from their equivalents in purple membrane but those of the protonated 13-cis states (K, L, and N) are less changed. The absorption maximum of the early M is about 4 nm to the red from that of the late M, and its amplitude is larger (Figure 2B). The measured spectra were fitted with linear combinations of the calculated difference spectra (Figure 2C,D) until the residuals were within ±2% of the amplitudes and without persistent structure. The weights used for the component spectra gave the kinetics of the intermediates. Figure 3 contains the calculated points as well as the best fits of the model K ↔ L ↔ M_1 → M_2 ↔ N ↔ O → BR *plus* N → BR we have used previously (Vârô & Lanyi, 1990a,b). Figure 3A,C shows the kinetics of K, L, and

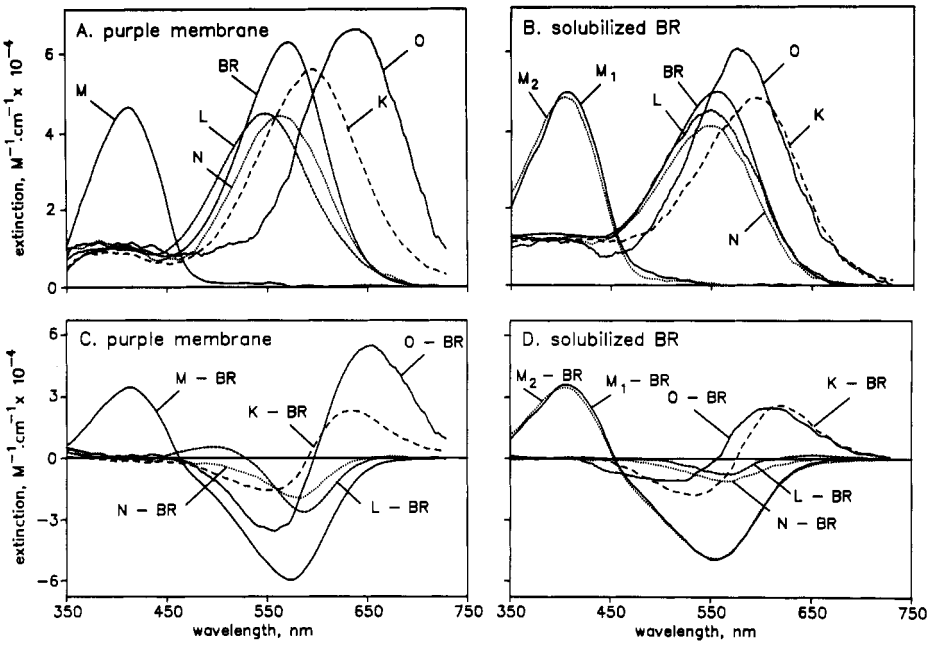

FIGURE 2: Calculated absorption spectra of the bacteriorhodopsin photocycle intermediates in purple membranes (A) and in Triton X-100 solubilized BR (B), and the corresponding difference spectra (C and D, respectively). The method of calculation and the assumptions are given in the text and in Váró and Lanyi (1990a). The spectra were smoothed by digital averaging.

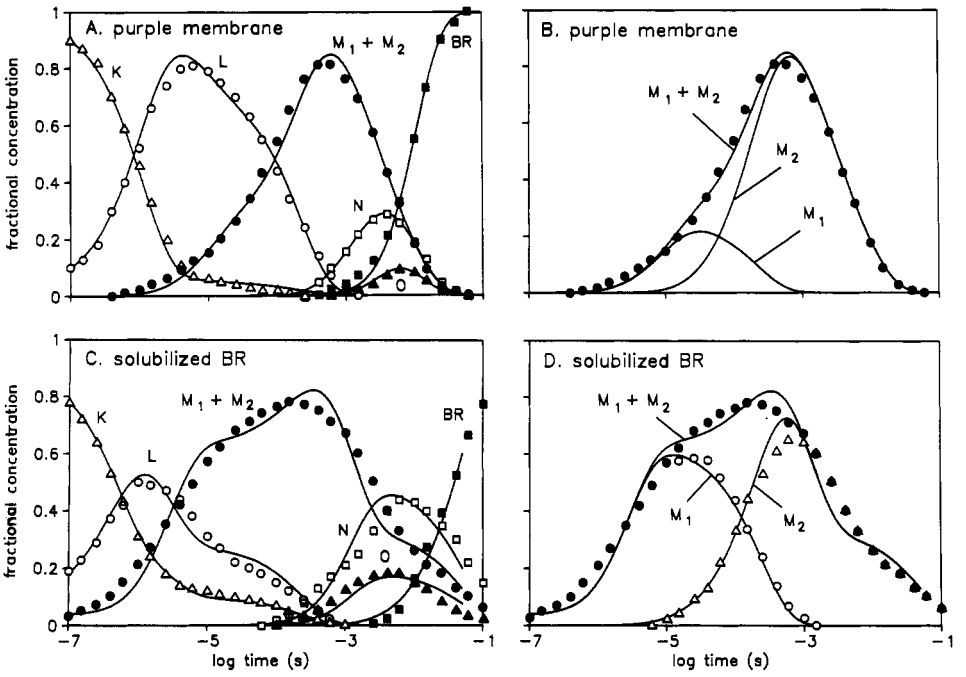

FIGURE 3: Time-dependent concentrations of the bacteriorhodopsin photocycle intermediates in purple membranes (A and B) and in Triton X-100 solubilized BR (C and D). The points represent the concentrations calculated from the different spectra; the lines describe the best fit of the model K ↔ L ↔ M_1 → M_2 ↔ N ↔ O → BR, *plus* N → BR. The rate constants (in s^{-1}) were the following (the values for solubilized BR are given in parentheses): $k_{KL} = 7.7 \times 10^5$ (1.43×10^6); $k_{LK} = 5.6 \times 10^5$ (5.0×10^5); $k_{LM_1} = 2.86 \times 10^4$ (3.3×10^5); $k_{M_1L} = 6.7 \times 10^4$ (1.43×10^5); $k_{M_1M_2} = 1.8 \times 10^4$ (6.7×10^3); $k_{M_2N} = 286$ (625); $k_{NM_2} = 170$ (400); $k_{NO} = 200$ (6.25×10^3); $k_{ON} = 416$ (1.7×10^4); $k_{NBR} = 200$ (0); and $k_{OBR} = 125$ (100). For clarity, the M_1 to M_2 reaction is shown in separate panels. In panels B and D, the lines designated with M_1 and M_2 describe the transient concentrations of M_1 and M_2 as calculated from the kinetics; in panel D, these quantities are given also from treating the time-dependent spectral shift of M as a conversion of M_1 into M_2 (points). (A and C) (△) K; (○) L; (●) $M_1 + M_2$; (□) N; (▲) O; (■) BR. (B and D) (●) $M_1 + M_2$; (○) M_1; (△) M_2.

M_1 *plus* M_2, N, and O, while panels B and D contain the kinetics of M_1 and M_2 as well as M_1 *plus* M_2. In Figure 3B, the kinetics of M_1 and M_2 are given from the kinetic calculations. In Figure 3D, we could calculate these also by fitting the two M − BR difference spectra (Figure 2D) to the measured spectra. This was possible because the difference between the two M spectra appeared as an easily recognized characteristic sharp feature in the residuals. Thus, a major difference in the data for BR in purple membrane and in detergent micelles was that in the former the two M species and their interconversion had to be inferred solely from fitting kinetic models to the calculated concentrations of K, L, and M but in the latter the existence of the two M species and the time course of the M_1 to M_2 transition were indicated also by a spectral shift. The kinetics and the spectral transition gave essentially the same time course for the reaction (Figure 3D). This is the first direct evidence that two M species appear consecutively in the photocycle. The data show that the rest

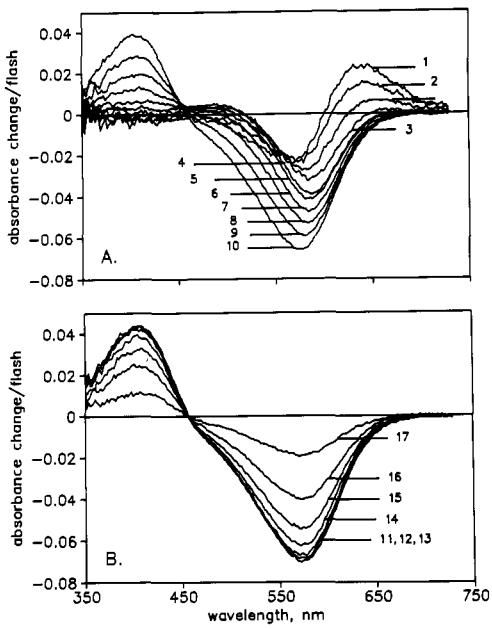

FIGURE 4: Measured time-resolved difference spectra for D96N bacteriorhodopsin in purple membranes. Delay times after photoexcitation are indicated by numbers. From 1 through 17, these were 100 ns, 250 ns, 600 ns, 1.5 μs, 4 μs, 10 μs, 25 μs, 60 μs, 150 μs, 400 μs, 1 ms, 2.5 ms, 6 ms, 15 ms, 40 ms, 250 ms, and 600 ms. Conditions: 20 nmol/mL BR, 100 mM NaCl, 50 mM phosphate buffer, pH 7.0, and 0.4 mM NaN_3.

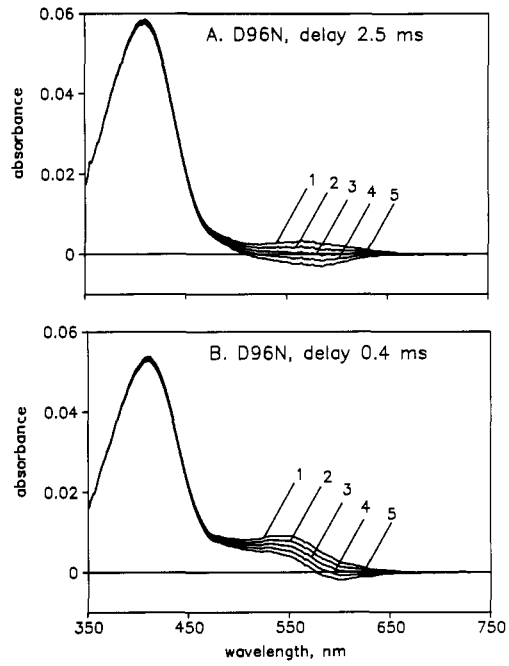

FIGURE 5: Resolution of two selected D96N bacteriorhodopsin difference spectra into components. Delay times: (A) 2.5 ms; (B) 0.4 ms. The spectra were measured as in Figure 4, but by averaging 2000 scans to reduce the signal/noise ratio. To the measured difference spectra was added the spectrum of BR (in Figure 6A) with the following scaling factors: curve 1, 0.1664; curve 2, 0.1632; curve 3, 0.1600; curve 4, 0.1568; curve 5, 0.1536. Since curve 3 in (A) is the spectrum of M without a contribution from other species (cf. text), we conclude that in this set of experiments the flash depleted 16.00% of the BR and at 2.5 ms only M was produced. Curve 3 in (B) represents a transient mixture of L, K, and M, but the contribution of K is not visible at this scale magnification.

of the kinetics are also changed by the solubilization: the rates of the L ↔ M_1 and the N ↔ O reactions are greatly accelerated, but that of the M_1 to M_2 reaction is slowed. Because of this, M_1 accumulates considerably more in solubilized BR than in purple membranes, and the M_1 to M_2 time constant dominates the decay kinetics of K and L. In the solubilized BR, the decay of M is distinctly nonexponential at pH 7 (Figure 3C,D) and at all pH values between 4 and 7 (not shown); this kind of kinetics is observed in purple membranes only at pH >8. The reason for the biphasic M decay in purple membranes is the effect of N accumulation on the M ↔ N equilibrium at slowed N decay rates (Otto et al., 1989). The intermediate O has little effect on this since the recovery curve for BR begins with the rise of O, arguing for an N → BR reaction which shunts O (Vârô et al., 1990). In solubilized BR, the reason appears to be different: here, rapid equilibration between M and N (time constant 1 ms) and N and O (time constant 45 μs) cause an equilibrium mixture to develop for M, N, and O, which then decay together with the time constant of the O → BR reaction (10 ms). The N → BR shunt does not seem to occur in solubilized BR.

Kinetic Analysis of the L to M Transition in a Bacteriorhodopsin Lacking a Protonable Residue at Position 96. In BR with the residue replacement D96N the rate of Schiff base reprotonation is linearly dependent on the external proton concentration (Holz et al., 1989; Butt et al., 1989a; Tittor et al., 1989), and the M state is much more stable than in wild-type BR. This simplifies the photocycle kinetics considerably and allows determination of the concentrations of L and M when these states reach an equilibrium but before M begins to decay. Under our usual conditions, i.e., at pH 7.0 with 100 mM NaCl, the decay time constant of about 2 s for M would have been inconveniently long for signal-averaging, and the measuring light would have produced a photostationary state containing a large amount of M. The M decay time constant was therefore adjusted to about 150 ms by adding 0.40 mM sodium azide. Azide partitions into the protein and replaces the missing D96 as proton donor without affecting Schiff base deprotonation (Tittor et al., 1989). We found that under these conditions the measuring light caused the accumulation of only about 4% M in the sample.

Figure 4 shows measured time-resolved difference spectra between 100 and 600 ms under these conditions. At the shorter delay times, the traces resemble those from wild-type BR (Figure 1A). After 0.6 ms, however, all of the measured spectra were of the same shape, and between 0.6 and 6 ms, they were also nearly identical in magnitude, indicating that in this time range M reached a quasi-equilibrium. The analysis of such spectra (cf. above) depends on using the right amount of depleted BR in calculating the component absorption spectra, and this value must be estimated from internal consistencies because it is not contained in the data. In the analysis below, we must be especially careful to correctly estimate the amount of depleted BR because its choice will influence the calculated amounts of L which contribute in the spectral mixtures, and therefore the conclusions. The following argument addresses this question.

Figure 5A shows a measured trace at 2.5 ms with various scaled amounts of BR spectra, in 2% increments relative to the optimal, added. We suggest on the basis of these traces that at 2.5 ms *the spectral contribution of any photointermediate other than M is negligible.* This is because by adding a BR spectrum with an appropriate scaling factor it is possible to obtain a spectrum for M in which there is no detectable contribution from a species which adsorbs to the red of the main peak (curve 3 in Figure 5A). The resulting M spectrum agrees well with previously obtained spectra (Lozier et al., 1975; Becher et al., 1978; Vârô & Lanyi, 1990a).

The only candidates for contaminating the measured spectrum at this delay time are K and L since the stability of M well beyond this time indicates that the formation of N has not yet begun. The absorption maxima of K and L differ sufficiently from BR (by 20–25 nm in either direction), however, to preclude removing a contribution of K or L by adding less BR spectrum than appropriate. Figure 5B illustrates this point. It shows an earlier difference spectrum, at 0.4 ms, which is expected to contain L and a small amount of K. In contrast with the traces in Figure 5A, in this case the addition of *no amount of BR spectrum will allow the absorption to smoothly decrease to the base line on the red side of the main peak and remain positive throughout.* If the assumption that the trace at 2.5 ms contains an undetectable amount of L is taken as correct, the fraction of BR depleted is given by that scaling factor which is Figure 5A produced the right spectrum for M (in this case 0.1600). With this value, we can calculate (cf. below) that at 0.4 ms (Figure 5B) the molar ratio of L to M is 0.087. By manipulating the traces in Figure 5A further, we established that at 2.5 ms the signal/noise ratio would have allowed the detection of L at an L/M ratio of greater than 0.01.

Once the amount of depleted BR and the spectrum of M were thus defined, we could use two early difference spectra to calculate absorption spectra also for K and L (Figure 6A). The three spectra are very similar to those in wild-type BR (Figure 2A), although the maximum of K is somewhat red-shifted and the maximum of L is slightly blue-shifted. It was shown earlier (Soppa et al., 1989) that D96N bacteriorhodopsin has essentially the same spectrum as wild type. As above, the measured difference spectra under our usual conditions (100 mM NaCl/50 mM phosphate at pH 7.0) were decomposed into sums of the calculated difference spectra; the weighting factors which are the time-resolved fractional concentrations of the intermediates are shown in Figure 6B (symbols). The lines are the fits of the model $K \leftrightarrow L \leftrightarrow M_1 \rightarrow M_2 \rightarrow BR$. The intermediates N and O did not accumulate to detectable levels under these conditions and were left out of the model. As in wild-type BR (Figure 2A), the decay of both K and L contains two clearly separable components, and after 0.6 ms the amount of L approaches zero. Unlike in wild-type BR, however, a quasi-equilibrium developed between 0.6 and 6 ms under the conditions used, where little change in the concentrations (i.e., that of M) occurred.

In a model with one M and a reversible $L \leftrightarrow M$ reaction, the concentration ratio of L and M at the equilibrium will be k_{ML}/k_{LM}. Since the upper limit for the L/M molar ratio at the equilibrium is 0.01 (Figure 5A), the L to M reaction would have to be essentially unidirectional. This model therefore does not explain the nonexponential kinetics of the L to M transition (Figure 6B). With two M states and reversibility allowed for both the L to M_1 and the M_1 to M_2 reactions, the concentration ratio at equilibrium will be

$$\frac{[L]}{[M_1] + [M_2]} = \frac{k_{M_1L}}{k_{LM_1}(1 + k_{M_1M_2}/k_{M_2M_1})} \quad (1)$$

Since the traces at 2.5 ms provide an estimate of 0.01 for the upper limit of the concentration ratio at the equilibrium (Figure 5A), the maximal value of $k_{M_2M_1}$ is 100 s^{-1}. This is equivalent to a forward/reverse ratio of at least 200 for the rate constants in the M_1 to M_2 reaction, and a decrease of $\geq$13.1 kJ/mol in ΔG at this step.

We have repeated these experiments with the D96N bacteriorhodopsin under the conditions used by Ames and Mathies (1990), as well as by Alshuth and Stockburger (1986) and

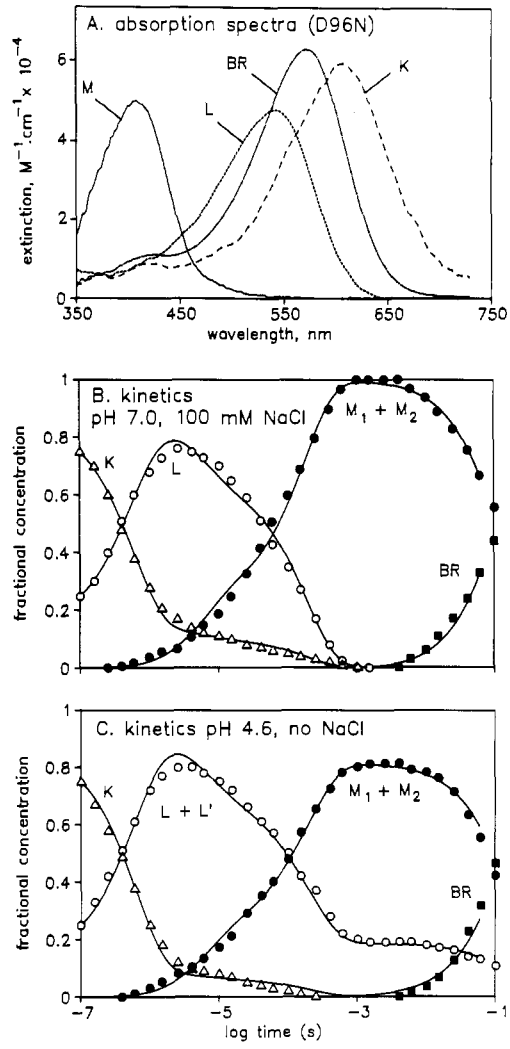

FIGURE 6: Calculated absorption spectra of the photointermediates of D96N bacteriorhodopsin (A) and the kinetics at pH 7 in the presence of NaCl (B) and at pH 4.6 in the absence of NaCl (C). Phosphate buffer (50 mM) was present under both conditions. Lines and symbols as in Figures 2 and 3; data in (A) and (B) from the experiments described in Figure 4. The extinctions were calculated with the assumption that the extinction of the D96N bacteriorhodopsin is the same as in wild type. In (B), the model used was $K \leftrightarrow L \leftrightarrow M_1 \rightarrow M_2 \rightarrow BR$. Symbols: (△) K; (○) L; (●) $M_1 + M_2$; (■) BR. The rate constants were the following (in s^{-1}): $k_{KL} = 1.4 \times 10^6$, $k_{LK} = 2.2 \times 10^5$, $k_{LM_1} = 5.0 \times 10^4$, $k_{M_1L} = 1.0 \times 10^5$, $k_{M_1M_2} = 2.0 \times 10^4$, and $k_{M_2BR} = 6.7$. In (C), the model was $K \leftrightarrow L \leftrightarrow M_1 \rightarrow M_2 \rightarrow BR$ *plus* $M_2 \leftrightarrow L'$. Symbols: (△) K; (○) L + L'; (●) $M_1 + M_2$; (■) BR. The rate constants were the following (in s^{-1}): $k_{KL} = 1.4 \times 10^6$, $k_{LK} = 1.25 \times 10^5$, $k_{LM_1} = 4.0 \times 10^4$, $k_{M_1L} = 1.0 \times 10^5$, $k_{M_1M_2} = 2.0 \times 10^4$, $k_{M_2L'} = 4.5 \times 10^3$, $k_{L'M_2} = 2.0 \times 10^4$, and $k_{M_2BR} = 6.7$.

Diller and Stockburger (1988), who reported from time-resolved resonance Raman measurements that the L/M ratio approached a nonzero value. All conditions used by these groups were duplicated except two: we used far less intensity for photoexcitation (and cycled only 12–16% of the BR per flash rather than near 50%), and the excitation was with a subnanosecond flash rather than with a light pulse which lasted from several microseconds to hundreds of microseconds. The former was to avoid nonlinear effects. The latter was to avoid exciting the early intermediates and to allow resolving the kinetics on the microsecond time scale. The following was reported. (1) In 3 M KCl, 0.5 m KNO_3, and 10 mM HEPES, pH 7.0 at 30 °C, the L/M ratio at 1 ms after photoexcitation was shown as about 0.2 [Figure 5C in Ames and Mathies (1990)]. The L amplitudes after 2–3 ms were close to but not quite zero, and the data were fitted to the model $L \leftrightarrow M \leftrightarrow$

N which predicted a constant L/M ratio during the rest of the photocycle. However, in our experiments (where 0.3 mM azide was also included), a contribution from L at 1 ms was just detectable, and the L/M ratio at 2.5 ms was as unmeasurably small as under the conditions in Figure 5A in this report (not shown). (2) In 50 mM phosphate buffer at pH 4.6, in the absence of NaCl, and L/M ratio of about 0.5 which remained constant at least up to 5 ms was reported [Figure 12 in Alshuth and Stockburger (1986)]. The model chosen was L ↔ M → BR, but later it was modified to include a second L state which originated from a second BR species (Diller & Stockburger, 1988). At this pH, the M decay was rapid enough for our measurements even without added azide. Under these conditions, we also detected a large amount of L-like species which coexisted with M until the end of the photocycle. We could fit the difference spectra with the component spectra obtained in the presence of NaCl (Figure 6A), and obtained the kinetics described in Figure 6C where the L/M ratio reached 0.23 at 1 ms and remained constant.

Thus, the model which fit the data in the presence of NaCl had to be modified to fit the data at pH 4.6 without salt. The following two modifications did not produce satisfactory fits: (1) increasing the rate of the back-reaction $M_2 \rightarrow M_1$ (at the large reverse rate required, this simplified the model to L ↔ M → BR); in this model, the observed biphasic L decay with a break at 0.1 ms (Figure 6C) will not occur, and K will not reach zero as long as L is present; (2) introducing a second L in an equilibration reaction with either L or M_1; this will not prolong the lifetime of L beyond that of M_1. The simplest model which did explain the results was K ↔ L ↔ M_1 → M_2 → BR as before, but with the addition of a second L, spectroscopically not different from the first, in an equilibration reaction with M_2. The line in Figure 6C is the best fit of this model.

Discussion

A description of the problems with models containing a single photocycle and only unidirectional reactions was given by Nagle et al. (1982). In view of these problems, several authors have attributed the observed multiexponential rise and decay kinetics, such as in Figure 3, to two simultaneous photocycles with similar steps but different microscopic rate constants. This model leads to at least two kinds of internal inconsistencies, however: (1) The amplitudes of the kinetic components do not agree (Vârô & Lanyi, 1990b). Up to the appearance of N, all the rise and decay rates are well separated from one another. In such a situation, the amplitudes associated with all of the reactions in a single pathway must be approximately equal because they describe the fraction of the reaction which proceeds through that pathway. Thus, it should be possible to divide the observed time constants into two sets, each with a characteristic common amplitude. There are no combinations of time constants and amplitudes for M rise and M decay, however, either in our data or in those of others (Scherrer & Stoeckenius, 1985; Butt et al., 1989b; Vârô & Lanyi, 1990a,b; this report), which show such a consistency. The problem is readily discerned under the conditions of the experiment in Figure 3A, where the decay of K contains a fast and a slow component in a roughly 15/1 amplitude ratio, while the two decay components observable for L are in a roughly 2/1 ratio. (2) Some of the time constants argue against consecutive reactions. Under some conditions [e.g., in solubilized BR (Figure 3C) and in BR films at lower humidities (Vârô & Lanyi, 1990a)], the slower of the time constants for the decay of K and L are very similar. This means that in a model with unidirectional reactions, in at least one of the pathways K and L cannot occur sequentially. In view of these complications, we feel that the multiexponential rates are better explained by the existence of reverse reactions; these will contribute an additional time constant for every reaction to which the process is kinetically connected. In such a model, the observed time constant and amplitude of a reaction are not independent of one another as both are determined by the microscopic rate constants. When conditions are examined where these rate constants are individually changed, simultaneous and self-consistent changes in the time constants and amplitudes will argue for valicity of the model with reversible reactions. This kind of self-consistency for temperature- and humidity-dependent shifts was indeed observed (Vârô & Lanyi, 1990a, 1991).

The results in this report, both spectroscopic and kinetic, strongly confirm the requirement for an irreversible $M_1 \rightarrow M_2$ step in the photocycle. The stabilization of M in the D96N bacteriorhodopsin allowed the unambiguous description of the late part of the L decay kinetics. We found that, as reported before, the concentration of L approached zero while the transient concentration of M was maximal, even though the L to M transition was best explained by a reversible reaction with similar forward and reverse rate constants. This confirmed the kinetic and discrepancy which necessitated introducing the $M_1 \rightarrow M_2$ reaction.

The data resolve an important disagreement in the kinetics of L decay as measured by spectroscopic features in resonance Raman and in the visible. The discrepancy appears to originate from the experimental conditions rather than the nature of the measurements. We reproduced, at least qualitatively, the results of Alshuth and Stockburger (1986) and Diller and Stockburger (1988) at pH 4.6 in the absence of NaCl. As the latter authors suggested, the explanation of the persistance of L under these conditions is best explained by the presence of a second L species, L′. The model we suggest is the same as in the presence of salt at pH 7, but in which L′ is in equilibrium with M_2. This is supported by the fact that after 1 ms under these conditions the ratio of L′ to M_2 remains constant (Figure 6C). The molecular explanation for L′ is not yet clear. Direct reprotonation of M_2 from the medium, such as catalyzed by azide in D96N, would accelerate the recovery of BR rather than cause the accumulation of an L-like state. It is more likely that the additional L represents the reversible reprotonation of the Schiff base from a residue other than D96. Unlike D96, however, this residue cannot be readily protonated from a third group or the medium, and therefore L′ decays either only via M_2 or directly, but in that case not more rapidly than M_2.

In purple membrane, the two M species appear to have the same absorption spectrum, and the $M \rightarrow M_2$ reaction is spectroscopically invisible. We found, however, that in monomeric BR the maximum in the M spectrum shifted at the same time that the kinetic analysis required the M_1 to M_2 transition. The interpretation of this shift as an interconversion between two M states with somewhat different spectra (Figures 2B and 3D) is the simplest explanation for the data. Interestingly, two kinetically resolved maxima for M (405 and 412 nm) were obtained also in BR-containing cell envelope vesicles with applied protonmotive force, and in deionized purple membrane sheets reconstituted with organometallic cations (Mathew et al., 1985). The relevance of these findings to the model proposed here is not clear.

The results show that the $M_1 \rightarrow M_2$ transition is essentially irreversible; i.e., it proceeds with a large free energy decrease. We had assumed a value of −17 kJ/mol in order to balance

the −180 mV of protonmotive force produced by the pump (Vârô & Lanyi, 1991). The results here indicate that it is at least −13 kJ/mol. Thus, this proposed coupling step also provides the rectification which ensures irreversibility of the pump.

References

Alshuth, T., & Stockburger, M. (1986) *Photochem. Photobiol. 43*, 55–66.

Ames, J. B., & Mathies, R. A. (1990) *Biochemistry 29*, 7181–7190.

Aton, B., Doukas, A. G., Callender, R. H., Becher, B., & Ebrey, T. G. (1977) *Biochemistry 16*, 2995–2999.

Becher, B., Tokunaga, F., & Ebrey, T. G. (1978) *Biochemistry 17*, 2293–2300.

Bitting, H. C., Jang, D.-J., & El-Sayed, M. A. (1990) *Photochem. Photobiol. 51*, 593–598.

Braiman, M. K., Ahl, P. L., & Rothschild, K. J. (1987) *Proc. Natl. Acad. Sci. U.S.A. 84*, 5221–5225.

Braiman, M. S., Mogi, T., Marti, T., Stern, L. J., Khorana, H. G., & Rothschild, K. J. (1988) *Biochemistry 27*, 8516–8520.

Butt, H.-J., Fendler, K., Dér, A., & Bamberg, E. (1989a) *Biophys. J. 56*, 851–859.

Butt, H. J., Fendler, K., Bamberg, E., Tittor, J., & Oesterhelt, D. (1989b) *EMBO J. 8*, 1657–1663.

Chernavskii, D. S., Chizhov, I. V., Lozier, R. H., Murina, T. M., Prokhorov, A. M., & Zubov, B. V. (1989) *Photochem. Photobiol. 49*, 649–653.

Dancshazy, Zs., Govindjee, R., & Ebrey, T. G. (1988) *Proc. Natl. Acad. Sci. U.S.A. 85*, 6358–6361.

Dencher, N. A., & Heyn, M. P. (1978) *FEBS Lett. 96*, 322–326.

Dencher, N. A., Kohl, K. D., & Heyn, M. P. (1983) *Biochemistry 22*, 1323–1334.

Dencher, N. A., Dresselhaus, D., Zaccai, G., & Büldt, G. (1989) *Proc. Natl. Acad. Sci. U.S.A. 86*, 7876–7879.

Diller, R., & Stockburger, M. (1988) *Biochemistry 27*, 7641–7651.

Engelhard, M., Gerwert, K., Hess, B., Kreutz, W., & Siebert, F. (1985) *Biochemistry 24*, 400–407.

Fodor, S. P., Ames, J. B., Gebhard, R., van der Berg, E. M., Stoeckenius, W., Lugtenburg, J., & Mathies, R. A. (1988a) *Biochemistry 27*, 7097–7101.

Fodor, S. P., Pollard, W. T., Gebhard, R., van den Berg, E. M., Lugtenburg, J., & Mathies, R. A. (1988b) *Proc. Natl. Acad. Sci. U.S.A. 85*, 2156–2160.

Gerwert, K., & Siebert, F. (1986) *EMBO J. 5*, 805–811.

Gerwert, K., Rodriquez-Gonzales, R., & Siebert, F. (1985) in *Time-resolved Vibrational Spectroscopy* (Laubereau, A., & Stockburger, M., Eds.) pp 263–268, Springer-Verlag, Berlin.

Gerwert, K., Hess, B., Soppa, J., & Oesterhelt, D. (1989) *Proc. Natl. Acad. Sci. U.S.A. 86*, 4943–4947.

Gerwert, K., Souvignier, G., & Hess, B. (1990a) *Proc. Natl. Acad. Sci. U.S.A. 87*, 9774–9778.

Gerwert, K., Hess, B., & Engelhard, M. (1990b) *FEBS Lett. 261*, 449–454.

Hanamoto, J. H., Dupuis, P., & El-Sayed, M. A. (1984) *Proc. Natl. Acad. Sci. U.S.A. 81*, 7083–7087.

Hasselbacher, C. A., & Dewey, T. G. (1986) *Biochemistry 25*, 6236–6243.

Henderson, R., Baldwin, J. M., Ceska, T. A., Zemlin, F., Beckmann, E., & Downing, K. H. (1990) *J. Mol. Biol. 213*, 899–929.

Holz, M., Drachev, L. A., Mogi, T., Otto, H., Kaulen, A. D., Heyn, M. P., Skulachev, V. P., & Khorana, H. G. (1989) *Proc. Natl. Acad. Sci. U.S.A. 86*, 2167–2171.

Kouyama, T., Nasuda-Kouyama, A., Ikegami, A., Mathew, M. K., & Stoeckenius, W. (1988) *Biochemistry 27*, 5855–5863.

Lozier, R. H., Bogomolni, R. A., & Stoeckenius, W. (1975) *Biophys. J. 15*, 955–963.

Mathew, M. K., Helgerson, S. L., Bivin, D., & Stoeckenius, W. (1985) *Biophys. J. 47*, 323a.

Nagle, J. F., & Mille, M. (1981) *J. Chem. Phys. 74*, 1367–1372.

Nagle, J. F., Parodi, L. A., & Lozier, R. H. (1982) *Biophys. J. 38*, 161–174.

Oesterhelt, D., & Stoeckenius, W. (1974) *Methods Enzymol. 31*, 667–678.

Otto, H., Marti, T., Holz, M., Mogi, T., Lindau, M., Khorana, H. G., & Heyn, M. P. (1989) *Proc. Natl. Acad. Sci. U.S.A. 86*, 9228–9232.

Parodi, L. A., Lozier, R. H., Bhattacharjee, S. M., & Nagle, J. F. (1984) *Photochem. Photobiol. 40*, 501–512.

Pettei, M. J., Yudd, A. P., Nakanishi, K., Henselman, R., & Stoeckenius, W. (1977) *Biochemistry 16*, 1955–1959.

Scherrer, P., & Stoeckenius, W. (1985) *Biochemistry 24*, 7733–7740.

Schulten, K., Schulten, Z., & Tavan, P. (1984) in *Information and Energy Transduction in Biological Membranes* (Bolis, A., Helmreich, H., & Passow, H., Eds.) pp 113–131, Alan R. Liss, Inc., New York.

Smith S. O., Lugtenburg, J., & Mathies, R. A. (1985) *J. Membr. Biol. 85*, 95–109.

Smith, S. O., Courtin, J., van der Berg, E., Winkel, C., Lugtenburg, J., Herzfeld, J., & Griffin, R. G. (1989) *Biochemistry 28*, 237–243.

Soppa, J., & Oesterhelt, D. (1989) *J. Biol. Chem. 264*, 13043–13048.

Soppa, J., Otomo, J., Straub, J., Tittor, J., Meessen, S., & Oesterhelt, D. (1989) *J. Biol. Chem. 264*, 13049–13056.

Stern, L. J., Ahl, P. L., Marti, T., Mogi, T., Dunach, M., Berkovitz, S., Rothschild, K. J., & Khorana, H. G. (1989) *Biochemistry 28*, 10035–10042.

Tittor, J., Soell, C., Oesterhelt, D., Butt, H.-J., & Bamberg, E. (1989) *EMBO J. 8*, 3477–3482.

Vârô, G., & Lanyi, J. K. (1990a) *Biophys. J. 59*, 313–322.

Vârô, G., & Lanyi, J. K. (1990b) *Biochemistry 29*, 2241–2250.

Vârô, G., & Lanyi, J. K. (1991) *Biochemistry* (following paper in this issue).

Vârô, G., Duschl, A., & Lanyi, J. K. (1990) *Biochemistry 29*, 3798–3804.

Zimányi, L., Keszthelyi, L., & Lanyi, J. K. (1989) *Biochemistry 28*, 5165–5172.